Breaking the limit of lignin monomer production via cleavage of interunit carbon-carbon linkages

Lin Dong, Longfei Lin, Xue Han, Xiaoqin Si, Xiaohui Liu, Yong Guo, Fang Lu, Svemir Rudić, Stewart F. Parker, Sihai Yang and Yanqin Wang

Published version information

Citation: L Dong et al. "Breaking the limit of lignin monomer production via cleavage of interunit carbon–carbon linkages." Chem, vol. 5, no. 6 (2019): 1521-1536.

DOI: 10.1016/j.chempr.2019.03.007

Breaking the limit of lignin monomer production *via* cleavage of interunit carbon-carbon linkages

Lin Dong[1,5], Longfei Lin[2,5], Xue Han[2], Xiaoqin Si[3], Xiaohui Liu[1], Yong Guo[1]*, Fang Lu[3], Svemir Rudić[4], Stewart F. Parker[4], Sihai Yang[2]* and Yanqin Wang[1,6]*

[1]Key Laboratory for Advanced Materials and Joint International Research Laboratory of Precision Chemistry and Molecular Engineering, Feringa Nobel Prize Scientist Joint Research Center, Research Institute of Industrial Catalysis, School of Chemistry and Molecular Engineering, East China University of Science and Technology, Shanghai, 200237 (China)
[2]School of Chemistry, the University of Manchester, Manchester, M13 9PL (UK)
[3]State Key Laboratory of Catalysis, Dalian Institute of Chemical Physics, Chinese Academy of Sciences, Dalian National Laboratory for Clean Energy, Dalian 116023 (China)
[4]ISIS Facility, STFC Rutherford Appleton Laboratory, Chilton, Oxfordshire, OX11 0QX (UK)

[5]These authors contribute equally to the work.
[6]Lead Contact
*Correspondence: guoyong@ecust.edu.cn
Sihai.Yang@manchester.ac.uk
wangyanqin@ecust.edu.cn

SUMMARY

Conversion of lignin into monocyclic hydrocarbons as commodity chemicals and drop-in fuels is a highly desirable target for biorefineries. However, this is severely hindered by the presence of stable interunit carbon-carbon linkages in native lignin and those formed during lignin extraction. Herein, we report a new multifunctional catalyst Ru/$NbOPO_4$ that achieves the first example of catalytic cleavage of both interunit C-C and C-O bonds in one-pot lignin conversions, yielding 124-153% of monocyclic hydrocarbons; that is 1.2-1.5 times those yields obtained from the established nitrobenzene oxidation method. This catalyst also exhibits high stability and selectivity (up to 68%) to monocyclic arenes over repeated cycles. The mechanism of the activation and cleavage of 5-5 C-C bonds in biphenyl, as a lignin model adopting the most robust C-C linkages, has been revealed *via in situ* inelastic neutron scattering, coupled with modelling. This study breaks the conventional theoretical limit on lignin monomer production.

INTRODUCTION

Lignin, accounting for 15-40 wt% of lignocellulosic biomass, is the most abundant source of renewable aromatics on earth.[1-4] The heavily branched 3D network of lignin is constructed from methoxylated phenylpropanoid subunits bridged by various interunit C-O and C-C linkages (accounting for approximately 70% and 30%, respectively) in a completely random order (Figure 1 and Figure S1).[5-7] C-C bonds have notably higher dissociation energy (226-494 kJ mol^{-1}) than those of C-O bonds (209-348 kJ mol^{-1}) in lignin (Table S1).[6] Owing to its highly robust polymeric structure, the conversion of lignin to small molecule arenes as commodity chemicals and fuel additives represents a significant challenge for industries and bio-refineries.

State-of-the-art processes usually undergo lignin depolymerisation *via* the cleavage of C-O bonds to obtain low-molecular-weight monomers, which can be sequentially upgraded to useful chemicals and fuels.[1,2] A great deal of effort has been devoted to developing strategies for the depolymerisation of lignin.[8-22] However, the primary products from these processes are mixtures of oxygen-containing compounds with high boiling points, which can hardly be separated using conventional distillation techniques. Moreover, the yields of lignin monomers are limited due to the presence of stable interunit C-C bonds within native lignin or those formed during lignin extraction.[23] Importantly, adding formaldehyde during the pre-treatment of biomass can effectively improve the yield of lignin monomers by preventing the interunit C-C coupling.[23,24] More interestingly, the emerging "lignin-first" approaches have shown productions of (near)theoretical amounts of phenolic monomers *via* solvolytic delignification, offering great promise for high-yield lignin depolymerisation.[4,21,22] However, the cleavage of intrinsic C-C bonds within native and technical lignin remains a longstanding challenge. Very recently, a CoS_2 catalyst has enabled the cleavage of C-C bonds in methylene-linked lignin models.[25] However, this catalyst has a limited structural stability and is inefficient to cleave the most robust 5-5 C-C linkages in lignin. Although lignin can be directly converted into volatile hydrocarbons *via* catalytic hydropyrolysis at typically 650 °C,[26-28] these processes are very energy consuming and deactivation of catalysts often occurs rapidly owing to the coke formation (up to 40%).[29-30]

Efficient catalytic cleavage of both interunit C-C and C-O linkages in lignin can maximise the lignin monomer production and thus is highly desirable. This is however a very challenging task and requires solutions based upon new multifunctional catalysts. Zeolite materials incorporating Brønsted acid sites can catalyse hydrocarbon cracking in petroleum refineries.[31,32] Phosphates-based materials containing strong Brønsted acid sites can protonate benzene rings and thus facilitate the cleavage of C-C bonds.[33,34] However, these

materials alone have poor activity in cleaving C-O bonds in lignin.[35] Meanwhile, the emerging NbO_x-supported catalysts have exhibited unique activities in cleaving C-O bonds in biomass to yield fully deoxygenated compounds.[36]

Here, we report a mesoporous multifunctional catalyst, $Ru/NbOPO_4$, which combines the NbO_x species and phosphates containing strong Brønsted acid sites and thus enables the efficient cleavage of both interunit C-O and C-C linkages in lignin. Significantly, the one-pot conversion of lignin over $Ru/NbOPO_4$ integrates the depolymerisation of lignin, the hydrogenolysis of depolymerised compounds and the cleavage of interunit C-C linkages, and achieves optimal production of monocyclic hydrocarbons. Theoretical yields of intrinsic lignin monomers have been determined from the established nitrobenzene oxidation (NBO) method (Note S1)[23, 37, 38] and serve as the 100 % standard in this report. Here, ratio of molar yields (RMY) is defined as (molar yield of monocyclic compounds over $Ru/NbOPO_4$) / (molar yield of monocyclic compounds from NBO) × 100%. When RMY above 100% is obtained, it suggests the recovery of additional monocyclic compounds from depolymerised dimer and oligomer products *via* the cleavage of interunit C-C linkages (Figure 1). The one-pot conversion of lignin over the $Ru/NbOPO_4$ catalyst has produced liquid monocyclic hydrocarbons with a RMY up to 153% as well as an exceptional arene selectivity of 68%. Furthermore, the unique activity of $Ru/NbOPO_4$ to crack the interunit C-C bonds has been confirmed in lignin dimer models (*e.g.*, biphenyl, diphenylmethane and diphenylethane), where high yields of monocyclic aromatics have been obtained. A combined inelastic neutron scattering (INS) and density functional theory (DFT) analysis unambiguously confirmed the strong adsorption with preferred orientation, activation and hydrogenolysis of biphenyl on the surface of $Ru/NbOPO_4$. To the best of our knowledge, this is the first example of using INS/DFT to study the mechanism of C-C bond activation in biomass conversions.

RESULTS

One-pot conversion of lignin into monocyclic hydrocarbons

Mesoporous $NbOPO_4$ was prepared from a hydrothermal reaction and a loading of 5 wt% Ru conducted *via* wetness impregnation (Note S2). The total acid amount and BET surface area of activated $Ru/NbOPO_4$ have been determined as 980 μmol g^{-1} and 235 m^2 g^{-1}, respectively, and the pore size distribution is centred at 3.5 nm (Figure S2). The mesopores and high porosity of the catalyst can promote reactions taking place at the solid-solid interface and have positive effect on mass transfer of substrates/reaction intermediates. Kraft lignin, typically produced from chemical pulping processes, has a highly-condensed and cross-linked (*via* interunit C-C bonds) network. Its intrinsic monomer units have been determined as 1040 μmol g^{-1} from the NBO method (Tables S2 and S3), which is widely used in literature as a standard protocol to analyse lignin monomers connected by C-O bonds (including but not limited to β-O-4 linkage).[23, 38, 39] The C-C linkage in lignin cannot be cleaved in the NBO method, thus making the comparison straightforward for the present study. It has been reported that the theoretical amount of lignin monomers coincides with the square of the fraction of ether bonds in the lignin structure, and that of birch lignin varies from 45% to 58%.[7,22] Using the NBO method, based on the molar content of S, G and H units in birch lignin, the maximum amount of lignin monomers is within the range of 52%-57% (Table S2 entry 4), highly consistent with the reported results. The one-pot conversion of Kraft lignin was first tested over the $Ru/NbOPO_4$ catalyst in dodecane at 310 °C under 0.5 MPa H_2 for 40 h. Interestingly and surprisingly, a very high yield of monocyclic hydrocarbons (1594 μmol g^{-1} / 14.5 wt%) was obtained with a C_6–C_9 arene selectivity of 68% (Table 1, entry 1; Table S4, entry 4; Table S5). This gives a RMY of 153%, indicating a 53% additional recovery of monocyclic hydrocarbons *via* the cleavage of interunit C-C linkages in Kraft lignin. Next, enzymic corncob, pine and birch lignin (representing grasses, softwood and hardwood lignin, respectively, Table S2 and Note S3) were employed as feedstocks (Table 1, entries 3-5; Table S6). The RMY for conversions of enzymic, pine and birch lignin were 147%, 151% and 124%, respectively, confirming the cleavage of interunit C-C linkages in all cases. Importantly, high selectivities to monocyclic arenes were obtained throughout, ranging from 62% to 67%, demonstrating the general applicability of this multifunctional catalyst and one-pot approach to produce monocyclic arenes. In addition, the comparison of the activity and selectivity with early reported literatures in the one-pot conversion of lignin was also summarized in Figure S3 and Note S4.

Stability tests

To investigate the stability of $Ru/NbOPO_4$, three consecutive conversions of Kraft lignin were conducted using the recycled catalyst. Negligible changes on reaction yield or arene selectivity were observed (Figure 2 and Table S7). For example, the yield of monocyclic hydrocarbons and arene selectivity on the third run were 1588 μmol g^{-1} and 66%, comparable to those (1594 μmol g^{-1} and 68%) achieved with a fresh catalyst. The stability test was also conducted using 100 wt% catalyst loading in four consecutive recycling runs (Table S8, Note S5), where the catalytic activity reduced after the first run and remained the same for following runs. XRD, TEM and chemical analysis further confirmed the absence of notable structural change, aggregation of Ru particles and leaching of Ru, respectively, for the used catalyst (Figures S4 and S5 and Table S9). These results demonstrate the excellent stability of $Ru/NbOPO_4$ in this one-pot process. In addition, the effect of S elemenet in Kraft lignin was also studied by control experiments, suggesting that the S element in Kraft lignin has little effect on the catalytic activity (Table S10 and Note S6).

Analysis of the reaction pathways

To investigate the reaction pathways, the conversion of Kraft lignin was conducted at 250 °C for 20h (Table 1, entry 2; Table S4 and Note S7), and reaction intermediates were isolated and analysed by two-dimensional heteronuclear single-quantum coherence nuclear magnetic resonance (2D-HSQC-NMR). Compared with the raw lignin, the NMR signals for A (β-O-4 linkages), B (β-5 linkages) and C (β-β linkages) decreased significantly in the side-chain regions post the reaction, and the presence of G and H subunits in the reaction residue is negligible (Figure S6). Elemental analysis shows only a minor oxygen content (<0.8wt%) in the reaction intermediates, further suggesting the near complete oxygen removal during the initial reaction. Meanwhile, bicyclic aromatic hydrocarbons (*e.g.*, biphenyl, diphenylethane) were also detected (Figure S7), indicating that the activation and cleavage of interunit C-C bonds in depolymerised compounds requires additional energy input, consistent with the difference on their bond dissociation energies (Table S1). The mass yield of total monocyclic compounds at 250°C for 20h was only 10.1 wt% (Table 1 entry 2) and that can be increased to 14.5 wt% at 310°C for 40h *via* further cleavage of C-C linkages in depolymerised compounds.

Catalytic cleavage of C_5-C_5 linkages in lignin model compounds

Among all interunit C-C linkages in lignin, the 5-5 bond between two phenyl groups accounts for the highest portion in lignin (40-50% in softwood and 25-40% in hardwood based on all C-C linkages) and has the strongest dissociation energies of 481-494 kJ mol^{-1}. Therefore, biphenyl is selected for in-depth investigation as a model compound for C-C cleavage.[7, 40] To closely monitor the intermediates, the reaction was conducted at a reduced temperature of 280 °C (Figure 3). Initially, phenylcyclohexane (**4**) was found to accumulate rapidly to 73% within 1h, and then gradually converted to benzene (**1**) and cyclohexane (**2**) as the reaction proceeded. This indicates that the partial hydrogenation of biphenyl occurred to activate the C_5-C_5 linkage from the sp^2-sp^2 to sp^2-sp^3 bond, thus effectively reducing the bond dissociation energy. Similar product distribution was obtained when using (**4**) as the substrate, confirming (**4**) being the primary intermediate in the conversion of biphenyl (Figure S8). Interestingly, a small amount of bicyclohexyl (**5**) was observed after 2h and no further conversion of (**5**) occurred with prolonged reaction time. Indeed, no product was detected in the hydrogeolysis of (**5**) or dodecane under the same reaction conditions (Figs. 4a and 4b), indicating that $Ru/NbOPO_4$ has a poor activity to cleave the $C_{aliphatic}$-$C_{aliphatic}$ bonds although they have considerably lower bond dissociation energy. Comparison of the FTIR spectra of adsorbed biphenyl, (**4**), (**5**), and dodecane on $Ru/NbOPO_4$ shows that the catalyst has much weaker binding to aliphatic hydrocarbons than that to aromatic ones (Figure S9 and Note S8), indicating that the adsorption of substrates on the catalyst surface plays an important role on its activation.

Interestingly, small amounts of (1-methylcyclopentyl)-benzene (**6**) and (1-methylcyclopentyl)-cyclohexane (**7**) were also detected, indicating the presence of isomerisations in this one-pot process. The hydrogenation of biphenyl can generate phenylcyclohexene, which undergoes isomerisation to give (**6**). (**6**) can be further cracked into benzene (**1**) and methylcyclopentane (**3**) (Figure 5, Route 2). On the other hand, (**3**) can also be obtained from the isomerisation of (**2**) (Figure 5, Route 1 and Figure S10). Thus, the conversion of biphenyl over $Ru/NbOPO_4$ firstly undergoes a partial hydrogenation to (**4**) or phenylcyclohexene, which is then converted *via* three plausible routes (Figure 5). In route 1, (**4**) is directly cracked into (**1**) and (2); the minority of the latter is isomerised to (**3**). In route 2, biphenyl is firstly hydrogenated to phenylcyclohexene, followed by isomerisation and hydrogenation to produce (**6**), which is finally cracked to (**1**) and (**3**). In route 3, further hydrogenation of (**4**) produces (**5**), which cannot undergo further conversion. It worth noting that the isomerisation in routes 1 and 2 has very minor contribution to the final products, and the direct cracking of (**4**) in route 1 is the dominant pathway, resulting in the efficient production of monocyclic hydrocarbons.

To investigate the role of density of acid sites, the conversion of biphenyl over Ru/Nb_2O_5 has been conducted (Table 2 entries 2-3). Compared with $Ru/NbOPO_4$, Ru/Nb_2O_5 shows significantly reduced activity for C-C cleavage, with only 3.5% yield of monocyclic products. While on addition of trifluoromethanesulfonic acid, the yield of monocyclic greatly increased to 38.0%, confirming the important role of Brønsted acids. Another control experiment of the hydrogenolysis of biphenyl over the catalyst support, $NbOPO_4$, has been conducted under the same reaction condition, and no product was detected (Table 2 entry 4). This result indicates that Ru nanoparticles serving as active sites for the dissociation of hydrogen molecules is also important, consistent with those reported in literature.[41, 42]

The performance of $Pd/NbOPO_4$, $Pt/NbOPO_4$ and $Rh/NbOPO_4$ on C-C cleavage of biphenyl has also been tested (Table 2 entries 5-7). Over $Pd/NbOPO_4$, the yield of benzene and cyclohexane was 16.3% and 12.3%, respectively, lower than that of $Ru/NbOPO_4$ (24.4% and 19.1%, respectively) and the main product was bicyclohexyl (42.1%). Over $Pt/NbOPO_4$, the main product is also bicyclohexyl (54.2%), with 18.5% cyclohexane and 1.3% benzene. The notably stronger activity for hydrogenation over Pd and Pt-catalysts than Ru-catalysts[14, 43] has greatly promoted further hydrogenation of the primary reaction intermediate (phenylcyclohexane) and thus hindered the cleavage of C-C bonds, leading to low yields of monocyclic products. Over the $Rh/NbOPO_4$ catalyst, the yield of monocyclic products reached 39.4%, but the arene selectivity was significantly lower than that of $Ru/NbOPO_4$, indicating that $Rh/NbOPO_4$ can promote further hydrogenation of benzene into alkanes. Thus, the unique activity of Ru-based analogue is attributed to its moderate ability for hydrogenation to enable the partial hydrogenation of biphenyl to phenylcyclohexane, meanwhile to prevent any further hydrogenation of the intermediate and product. It is worth noting that all catalysts (Ru, Pd, Pt or $Rh/NbOPO_4$) are inactive for C-C cracking of bicyclohexyl under the same conditions.

HZSM-5 is widely used for cracking and hydrocracking processes in petroleum refineries,[44] and Ru/HZSM-5 has also been studied for the conversion of biphenyl (Table 2, entry 8). The yield of monocyclic hydrocarbons over Ru/HZSM-5 is only 8.8%, with phenylcyclohexane being the main product (57.3%), together with small amounts of C_1-C_4 products in the gas phases. This result gives sharp comparisons to $Ru/NbOPO_4$, which can effectively prevent the deep cracking of substrate/intermediates and thus lead to the optimal production of monocyclic arenes.

Catalytic cleavage of other C-C linkages in lignin model dimers

Conversions of diphenylmethane and diphenylethane, as the α-1 and β-1/β-5 lignin models, respectively, were also studied. The conversion of diphenylmethane gives benzene (31.7%) and toluene (10.8%) as two main products together with the presence of a small amount of ring-saturated products (Figure 4c). For diphenylethane, the main products are benzene and ethylbenzene (12.4% and 6.7%, respectively) with a small amount of toluene (2.7%) (Figure 4d). These results confirm that $Ru/NbOPO_4$ truly has activity for the selective and direct hydrogenolysis of $C_{aromatic}$-C bonds (Figure 4e). The carbon balance is 88~92% and the discrepancies are due to (i) the adsorption of substrate/intermediate/product on the catalyst surface, (ii) a small amount of alkanes products in gas phase, and (iii) small loss of product during the extraction and transfer of product during analysis.

INS studies on adsorption, activation and hydrogeolysis of biphenyl

The selective cleavage of interunit C–C linkages in depolymerised lignin components while maintaining the aromatic functionalities of phenyl rings leads to the optimal production of monocyclic arenes in this study. Direct visualisation of the interaction between adsorbed biphenyl and the catalyst ($Ru/NbOPO_4$) surface is crucial to understand the molecular details of adsorption, activation and hydrogenolysis of biphenyl into monocyclic hydrocarbons. INS is a powerful neutron spectroscopy technique to investigate the dynamics (particularly for the deformational and conformational modes) of biphenyl, and the DFT calculation of INS spectra is straightforward. Therefore, combined *in situ* INS and DFT calculations have been applied to investigate the molecular binding properties of the biphenyl-$Ru/NbOPO_4$ system to reveal the conversion mechanism of biphenyl.

The INS spectrum of bare $Ru/NbOPO_4$ catalyst gives a clean background with a broad feature centred at 1100 cm^{-1}, indicating the presence of surface hydroxyl groups (Figures S11 and S12 and Note S9). In comparison, on adsorption of biphenyl at 220 °C, the INS spectrum shows a significant increase in total intensity, demonstrating the binding of biphenyl to the catalyst surface (Figure S11). The INS spectrum of solid biphenyl was also collected and analysed *via* DFT calculations (Figure S13 and Table S11), allowing a full assignment of the spectral features for biphenyl.

Comparison of the difference of INS spectra before and after biphenyl adsorption on the catalyst (that is, signals for adsorbed biphenyl) and that of the solid biphenyl shows a number of marked changes (Figure 6a). Peaks at low energy (below 120 cm^{-1}), assigned to the translational and rotational modes of biphenyl, shift to lower energy with a continuum profile, suggesting that adsorbed biphenyl molecules are disordered over the catalyst surface with hindered motions as a result of the strong binding to the catalyst. The modes of C_5-C_5 out-of-plane and in-plane bending (135 and 189 cm^{-1}, respectively) have disappeared completely upon adsorption on the catalyst surface, suggesting that the biphenyl molecule adsorbed onto the catalyst with a flat position. Meanwhile, the peak at 443 cm^{-1} (assigned to C_2 and C_5 out-of-plane wagging) decreases significantly and shifts to higher energy at 488 cm^{-1} (Δ=45 cm^{-1}); this notable blue-shift is consistent with the strong binding of phenyl plane on catalyst surface. The intensities of deformational modes of benzene rings at 628, 736, 986 cm^{-1} also reduced dramatically. These results strongly indicate that both benzene rings of biphenyl adsorbed on the catalyst. Meanwhile, the wagging (677, 1100, 1281 cm^{-1}), scissoring (1215 cm^{-1}) and rocking (1480 cm^{-1}) modes of C-H groups on both benzene rings have disappeared and INS peaks at 913 cm^{-1} (C-H wagging), 1045 cm^{-1} (C-H rocking) and 1178 cm^{-1} (C-H scissoring) notably decreased in intensity. The peaks at 245 and 392 cm^{-1}, corresponding to the twisting mode of C-C bond within benzene rings, shift to 269 and 366 cm^{-1}, respectively. The peak at 331 cm^{-1} (assigned to the intra-ring stretching mode of benzene) shifts to lower energy at 313 cm^{-1} (Δ=18 cm^{-1}). These changes suggested that the adsorbed biphenyl molecules are partially protonated by the acid sites residing on the catalyst surface (*e.g.,* hydroxyls) and intermediate carbocation formed (Figure S10).[45] These results are in good agreement with *in situ* FTIR experiments where a red-shift (Δ=28 cm^{-1}) was observed for the C_5-C_5 stretching mode on adsorption (Figure S14 and Note S8).

The adsorbed biphenyl molecules on $Ru/NbOPO_4$ underwent a first catalytic conversion in H_2 at 170 °C for 6 min. Comparison of the INS spectra of the first reacted and adsorbed biphenyl shows a few changes (Figure 6b). The peaks at 736 and 986 cm^{-1} (ring deformational mode of phenyl group) have disappeared upon reaction in H_2, and the peaks at 269, 313 and 366 cm^{-1} shift to 275, 295 and 358 cm^{-1}, respectively, indicating the formation of phenylcyclohexane *via* the further hydrogenation of the intermediate carbocation. The spectrum for reacted catalyst also shows the appearance of several new features at 242, 432, 460, 512, 895, 1274, 1348 and 1456 cm^{-1}, which are all consistent with the spectrum of phenylcyclohexane. In contrast, the INS spectrum also confirms the absence of bicyclohexyl on catalyst surface (Figure S15), suggesting only one benzene ring on biphenyl is hydrogenated during the initial reaction.

To promote the further conversion of phenylcyclohexane, a second hydrogenation was carried out by feeding a H_2 (5%)/He stream at 270 °C for 6 min. The cell outlet was monitored continuously *via* mass spectrometry that confirmed the presence of benzene as the main product. Comparison of the INS spectra of the 1st and 2nd reacted biphenyl on $Ru/NbOPO_4$ shows an interesting observation (Figure 6c): the INS peaks for phenylcyclohexane significantly reduced in intensity (436, 496, 1348 and 1453 cm^{-1}) or completely disappeared (242, 464 and 895 cm^{-1}) on the 2nd reaction, indicating that high temperature greatly promoted the cleavage of C_5–C_5 bonds in adsorbed phenylcyclohexane on $Ru/NbOPO_4$. New features appeared at 609 and 980 cm^{-1}, and the peaks at 405, 702, 857 and 1185 increased in intensity, fully consistent with the formation of benzene.

To confirm the adsorption domain, INS data were also collected for biphenyl-adsorbed catalyst support, $NbOPO_4$ (Figure S16), and the INS spectra are fully consistent with that of $Ru/NbOPO_4$, indicating that the primary adsorption sites of $Ru/NbOPO_4$ reside on $NbOPO_4$ and Ru particles have little effect on adsorption. Similar observations have also been obtained from an *in situ* FTIR experiment (Figure S17). Furthermore, the conventional C-C cracking catalyst, HZSM-5, has also been selected for the study of biphenyl adsorption by INS and DRIFT (Figures S18, S19). The INS data confirms the strong binding of biphenyl on HZSM-5 surface and small differences between adsorbed biphenyl on HZSM-5 and $NbOPO_4$ were observed. The ring deformation mode of adsorbed biphenyl on $NbOPO_4$ observed at 628 cm^{-1} disappeared upon adsorption on HZSM-5. The C-H wagging mode of biphenyl at 677 cm^{-1} disappeared upon adsorption on $NbOPO_4$, while this is clearly visible for HZSM-5. *In situ* DRIFT data revealed a large red-shift (Δ = 100 cm^{-1}) for the C-H stretching mode of adsorbed biphenyl over $NbOPO_4$, while the red-shift is only by 10 cm^{-1} over HZSM-5 (Figure S19). These results confirm that $NbOPO_4$ shows stronger adsorption of biphenyl than HZSM-5.

The adsorption of key intermediate (phenylcyclohexane) on $NbOPO_4$ and HZSM-5 has also been studied by INS to reveal the origin on their distinct catalytic activities. The DFT-calculated INS spectrum of phenylcyclohexane has an excellent agreement with the experimental data (Figure S20, Table S12). Comparison of the difference INS spectrum before and after phenylcyclohexane adsorption on $NbOPO_4$ (that is, signals for adsorbed phenylcyclohexane) and that of the solid biphenyl shows a number of changes (Figure S21). Peaks at low energy (below 120 cm^{-1}), assigned to the translational and rotational modes of phenylcyclohexane, shift to lower energy

with a continuum profile, suggesting that the adsorbed phenylcyclohexane molecules are disordered over the catalyst surface with hindered motions as a result of the strong binding to the catalyst. A number of INS peaks of phenylcyclohexane decrease in intensity on adsorption on $NbOPO_4$, including bands at 297 cm^{-1} (wagging of C_2, C_4 and C_6 in benzene ring), 530 cm^{-1} (wagging of C_2 and C_5 in benzene ring), 848 cm^{-1} and 996 cm^{-1} (wagging of C-H groups on benzene ring), indicating that the adsorption of phenylcyclohexane is primarily *via* its benzene ring. The wagging modes (247 cm^{-1}) of C_7 and C_{10} of the cyclohexane ring has disappeared completely upon adsorption, and the intensities of C-C twisting modes (237 cm^{-1}) in the cyclohexane ring greatly reduced, indicating the hindrance of motion of the cyclohexane ring on adsorption. In contrast, the comparison of INS spectra of adsorbed phenylcyclohexane on HZSM-5 and that of solid phenylcyclohexane shows only small decreases on intensity of peaks at 247, 281 and 297 cm^{-1}. This result suggests that adsorbed phenylcyclohexane is weakly bound on the surface of HZSM-5 with similar motions to the solid state and can easily desorb. This is in excellent agreement with the catalysis result where phenylcyclohexane was obtained as the main product over the Ru/HZSM-5 catalyst. Thus, the INS study confirms that although biphenyl can strongly adsorb on both $NbOPO_4$ and HZSM-5, the former is also able to provide strong adsorption to the intermediate, phenylcyclohexane, thus leading to the selective C-C cleavage to produce monocyclic products (Figure S22).

This INS study has confirmed that (i) both benzene rings of biphenyl strongly adsorb on the catalyst surface with a flat orientation, and on adsorption, benzene rings are protonated and the intermediate carbocation formed; (ii) hydrogenation of one benzene ring of biphenyl occurs rapidly in the presence of H_2 to give phenylcyclohexane adsorbed on the catalyst *via* its phenyl group; (iii) C_5–C_5 bonds are then efficiently cleaved on $Ru/NbOPO_4$, and the volatile products readily desorb from the catalyst surface, thus preventing the further hydrogenation of reaction intermediates and products and driving the formation of arenes. Therefore, the catalytic conversion of biphenyl follows adsorption, binding, protonation, partial hydrogenation and cleavage of C_5–C_5 linkages, and the catalyst $Ru/NbOPO_4$ played an important role in the optimal production of monocyclic aromatics.

DISCUSSION

Much current research on lignin conversion is centred on its depolymerisation *via* cleavage of C-O bonds. Interunit C-C bonds have higher dissociation energies but their cleavage is critical if the production of low-molecular-weight commodity chemicals and jet-fuels from lignin is to be improved. A multifunctional catalyst, $Ru/NbOPO_4$, has been designed by integrating the Brønsted acid sites onto the emerging NbO_x support, coupled with the moderate hydrogenation ability of Ru centres, to enable the cleavage of both interunit C-O and C-C linkages to maximise the lignin monocyclic hydrocarbon production. Exceptional yields (up to 153%, comparing to intrinsic lignin monomer units) of monocyclic hydrocarbons have been obtained from the one-pot conversion of various types of lignin. This approach also shows complete removal of oxygen content from lignin and exhibits high selectivity to arene products. Detailed studies using lignin models, including biphenyl, diphenylmethane and diphenylethane, over multiple catalysts confirmed the unique activity of $Ru/NbOPO_4$ on the selective cleavage of interring C-C linkages. *In situ* inelastic neutron scattering and modelling studies confirm that the excellent activity of $Ru/NbOPO_4$ originates from a combination of strong adsorption and a synergistic effect between Ru, NbO_x species and acid sites on the catalyst surface. Ru particles, NbO_x species and acid sites promote the dissociation of hydrogen, the strong adsorption of substrates and intermediates, and the partial protonation and activation of adsorbed substrates (*e.g.,* biphenyl), respectively, thus driving the entire reaction.

Zeolite-based catalysts currently dominate the state-of-the-art petroleum refineries for hydrocarbons cracking and pyrolysis-based bio-refineries to produce small molecule feedstock chemicals.[31] Significantly, the activity of $Ru/NbOPO_4$ is distinct to conventional zeolite-based catalysts. This new one-pot process for lignin conversion offers efficient cleavage of both interunit C-C and C-O cleavages and effectively prevents the deep C-C cracking of low-molecular-weight products. Thus, it results in the isolation of desirable liquid C_6~C_9 monocyclic hydrocarbons under mild conditions and successfully breaks the conventional theoretical limit on lignin monomer production.

EXPERIMENTAL PROCEDURES

Catalytic reactions and analysis of products

The detailed reaction conditions are described in the figure captions and table footnotes. The one-pot conversion of lignin was conducted in a 25 mL stainless-steel autoclave reactor. In a typical reaction, lignin (0.10 g), catalyst (0.20 g), and dodecane (5 mL) were filled into the reactor, which was then sealed, purged three times with H_2 and charged to an initial pressure of 0.5 MPa with H_2. The reactor was heated to a target temperature and reaction conducted with magnetic stirring. After the reaction, the reactor was quenched in an ice-water bath, and reaction mixture centrifuged to separate the catalyst. The organic phase was qualitatively analysed by GC-MS (Agilent 7890A-5975C) and quantitatively analysed by GC-flame ionisation detector (Agilent 7890A) with a HP-5 column. Initial column temperature: 50°C (held for 5 min), raised at 10°C min^{-1} to 250°C (held for 1 min), total running time 26 min. Pentadecane was used as an internal standard for the quantification of the liquid products. For the stability test, after each reaction, the used catalyst was isolated by centrifugation, washed with ethanol to remove the unreacted lignin, and dried at 80 °C in air overnight before the next run. The theoretical yield of lignin monocyclic units is determined using the established nitrobenzene oxidation (NBO) method (Note S1).[23,37,38] The conversion of lignin models and product analysis were conducted using the same method.

Inelastic neutron scattering (INS) experiments

INS spectra were recorded on the TOSCA spectrometer at the ISIS Facility at the STFC Rutherford Appleton Laboratory (UK). TOSCA is an indirect geometry crystal analyser instrument that provides a wide dynamic range (16-4,000 cm^{-1}) with resolution optimised in the 50-2,000 cm^{-1} range[46]. All the INS spectra for the catalysis system were collected after the sample was cooled and stabilized at temperatures below 30 K.

In a typical experiment, the Ru/$NbOPO_4$ catalyst (22.84g) was loaded into a flow-type stainless steel cell that can also be used as a static cell with all valves closed. Similar amounts of catalysts were used for studies of $NbOPO_4$ and HZSM-5. The Ru/$NbOPO_4$ catalyst used here has a 5 wt% loading of Ru. The sample was heated at 300 ºC (5 ºC min^{-1} ramping) under He for 3 h to remove any remaining trace water before the experiment. The sample was cooled to room temperature and a weight loss of 0.89 g was noted, assigned to loss of adsorbed water. The activated catalyst was then reduced by heating under a H_2 flow at 250 ºC for 3 h. The samples were cooled to <30 K during data collection by a closed cycle refrigerator cryostat. The procedure of the *in situ* catalysis experiment with the INS measurements is summarised in Figure S23. To study the reaction mechanism, biphenyl was used as a 5-5 linked lignin model compound. Adsorption of biphenyl was carried out by flowing hot biphenyl vapour diluted in He (1.1 bar, 0.15 L min^{-1}; this flow condition was used throughout the study) over the catalyst at 220 ºC for 2.5 h, and the exhaust gas was monitored *via* mass spectrometry. Before the data collection, the cell was flushed using dry He to remove weakly bound biphenyl molecules. The adsorbed biphenyl underwent the first catalytic conversion in pure H_2 flow for 6 min at 170 ºC. The cell was then flushed with He to remove weakly bound products and free H_2, sealed and cooled for INS collection. After the data collection, H_2 (5%) was introduced to the cell for 6min at 270 ºC for the second catalytic reaction to occur and production of benzene was observed instantly by mass spectrometry. The cell was then flushed with He again, sealed and cooled for INS collection to detect the presence of possible reaction intermediates. INS spectra of pure solid compounds for both starting material and reaction products were collected at 10 K. The amount of each sample in the neutron beam is: 1.3g (biphenyl), 2.6g (phenylcyclohexane), 2.8g (bicyclohexyl) and 8.1g (benzene).

In situ diffuse reflectance infrared Fourier transform spectroscopy

The DRIFT spectra were recorded using a Nicolet NEXUS 670 FT-IR spectrometer equipped with an in situ reaction chamber and a liquid N_2 cooled high sensitivity MCT detector. Prior to the FTIR studies, about 20 mg of the catalysts was finely ground and placed in the chamber. The procedure of the in situ biphenyl adsorption experiment with the FTIR measurements is summarised in Figure S24. Before adsorption, the catalysts were activated in flowing He at 300 ºC for 1 h to remove any remaining trace water, then reduced in flowing H_2 at 250 ºC for 1 h and decreased to 220 ºC to collect the background spectra. For the adsorption of biphenyl, it was fed into the chamber by flowing biphenyl vapour in He for 0.5h, then, the chamber was flushed using dry He at 220 ºC for 1h to remove physical/weakly adsorbed molecules, and finally the spectra were recorded with a resolution of 4 cm^{-1} and an accumulation of 64 scans. For the adsorption of phenylcyclohexane, bicyclohexyl, and dodecane were conducted in the same method (Figure S9 and Note S8). All spectra were used after subtracting the background.

DATA AND SOFTWARE AVAILABILITY

The data supporting the findings of this study are available within the article, or available from the authors upon reasonable request.

SUPPLEMENTAL INFORMATION

Supplemental Information includes Supplemental Experimental Procedures, 24 figures, 12 tables, and 9 notes can be found with this article online at http://.

ACKNOWLEDGMENTS

This work was supported financially by the NSFC of China (No. 21832002, 21872050, 21808063, 91545103), the Science and Technology Commission of Shanghai Municipality (2018SHZDZX03), the Programme of Introducing Talents of Discipline to Universities (B16017) in China, the Fundamental Research Funds for the Central Universities (222201718003), and University of Manchester, the Royal Society and the EPSRC (EP/P011632/1) in the UK. We are especially grateful to STFC and ISIS Neutron Facility for access to the Beamline TOSCA. We thank S. Xu, Q. Xia, C. Goodway and M. Kibble for their help at the beamline. Computing resources (time on the SCARF cluster for the CASTEP calculations) was provided by STFC's e-Science facility.

AUTHOR CONTRIBUTIONS

L.D., X.H.L. and Y.G.: conduction of catalytic reactions and material characterisations. L. L., X.H., S.R. and S.F.P.: collection and analysis of INS data and DFT calculations. X.Q.S. and F.L.: collection and analysis of 2D-HSQC-NMR data. Y.G., S.Y. and Y.Q.W.: direction of the project and preparation of the manuscript.

DECLARATION OF INTERESTS

The authors declare no competing interests.

REFERENCES AND NOTES

1. Zakzeski, J., Bruijnincx, P.C.A., Jongerius, A.L., and Weckhuysen, B.M. (2010). The catalytic valorization of lignin for the production of renewable chemicals. Chem. Rev. *110,* 3552-3599.
2. Li, C., Zhao, X., Wang, A., Huber, G.W., and Zhang, T. (2015). Catalytic transformation of lignin for the production of chemicals and fuels. Chem. Rev. *115,* 11559-11624.
3. Ragauskas, A.J., Beckham, G.T., Biddy, M.J., Chandra, R., Chen, F., Davis, M.F., Davison, B.H., Dixon, R.A., Gilna, P., Keller, M., et al. (2014). Lignin valorization: improving lignin processing in the biorefinery. Science *344,* 1246843.
4. Schutyser, W., Renders, T., Bosch, S.V., Koelewijn, S.-F., Beckham, G.T., and Sels, B.F. (2018). Chemicals from lignin: an interplay of lignocellulose fractionation, depolymerisation, and upgrading. Chem. Soc. Rev. *47,* 852-908.
5. Xu, C.P., Arancon, R.A.D., Labidi, J., and Luque, R. (2014). Lignin depolymerisation strategies: towards valuable chemicals and fuels. Chem. Soc. Rev. *43,* 7485-7500.
6. Rinaldi, R., Jastrzebski, R., Clough, M.T., Ralph, J., Kennema, M., Bruijnincx, P.C.A., and Weckhuysen B.M. (2016). Paving the way for lignin valorisation: recent advances in bioengineering, biorefining and catalysis. Angew. Chem. Int. Ed. *55,* 8164-8215.
7. Yan, N., Zhao, C., Dyson, P.J., Wang, C., Liu, L.-T., and Kou, Y. (2008).

Selective degradation of wood lignin over noble-metal catalysts in a two-step process. ChemSusChem *1,* 626-629.
8. Rahimi, A., Ulbrich, A., Coon, J.J., and Stahl, S.S. (2014). Formic-acid-induced depolymerisation of oxidized lignin to aromatics. Nature *515,* 249-252.
9. Wu, X., Fan, X., Xie, S., Lin, J., Cheng, J., Zhang, Q., Chen, L., and Wang, Y. (2018). Solar energy-driven lignin-first approach to full utilization of lignocellulosic biomass under mild conditions. Nat. Catal. *1,* 772-780.
10. Sun, Z., Bottari, G., Afanasenko, A., Stuart, M.C.A., Deuss, P.J., Fridrich, B., and Barta, K. (2018). Complete lignocellulose conversion with integrated catalyst recycling yielding valuable aromatics and fuels. Nat. Catal. *1,* 82-92.
11. Deuss, P.J., Scott, M., Tran, F., Westwood, N.J., Vries, J.G., and Batra, K. (2015). Aromatic monocyclics by in situ conversion of reactive intermediates in the acid-catalyzed depolymerisation of lignin. J. Am. Chem. Soc. *137,* 7456-7467.
12. Lahive, C.W., Deuss, P.J., Lancefield, C.S., Sun, Z., Cordes, D.B., Young, C.M., Tran, F., Slawin., A.M.Z., Vries, J.G., Kamer, P.C.J., et al. (2016). Advanced model compounds for understanding acid-catalyzed lignin depolymerisation: identification of renewable aromatics and a lignin-derived solvent. J. Am. Chem. Soc. *138,* 8900-8911.
13. Stark, K., Taccardi, N., Bosmann, A. and Wasserscheid, P. (2010). Oxidative depolymerisation of lignin in ionic liquids. ChemSusChem *3,* 719-723.
14. Li, Y.D., Shuai, L., Kim, H., Motagamwalaet, A.H., Mobley, J.K., Yue, F., Tobimatsu, Y., Havkin-Frenkel, D., Chen, F., Dixon, R.A., et al. (2018). An "ideal lignin" facilitates full biomass utilization. Sci. Adv. *4,* eaau2968.
15. Rahimi, A., Azarpira, A., Kim, H., Ralph, J. and Stahl, S.S. (2013). Chemoselective metal-free aerobic alcohol oxidation in lignin. J. Am. Chem. Soc. *135,* 6415-6418.
16. Parsell, T., Yohe, S., Degenstein, J., Jarrell, T., Klein, I., Gencer, E., Hewetson, B., Hurt, M., Kim, J.I., Choudhari, H., et al. (2015). A synergistic biorefinery based on catalytic conversion of lignin prior to cellulose starting from lignocellulosic biomass. Green Chem. *17,* 1492-1499.
17. Klein, I., Saha, B., and Abu-Omar, M.M. (2015). Lignin depolymerisation over Ni/C catalyst in methanol, a continuation: effect of substrate and catalyst loading. Catal. Sci. Technol. *5,* 3242-3245.
18. Matson, T.D., Barta, K., Iretskii, A.V., and Ford, P. C. (2011). One-pot catalytic conversion of cellulose and of woody biomass solids to liquid fuels. J. Am. Chem. Soc. *133,* 14090-14097.
19. Song, Q., Wang, F., Cai, J., Wang, Y., Zhang, J., Yu, W., and Xu, J. (2013). Lignin depolymerisation (LDP) in alcohol over nickel-based catalysts via a fragmentation–hydrogenolysis process. Energy Environ. Sci. *6,* 994-1007.
20. Wang, X., and Rinaldi, R. (2013). A route for lignin and bio-oil conversion: dehydroxylation of phenols into arenes by catalytic tandem reactions. Angew. Chem. Int. Ed. *52,* 11499-11503.
21. Van den Bosch, S., Schutyser, W., Vanholme, R., Driessen, T., Koelewijn, S.-F., Renders, T., Meester, B.D., Huijgen, W.J.J., Dehaen, W., Courtin, C.M. et al. (2015). Reductive lignocellulose fractionation into soluble lignin-derived phenolic monocyclics and dimers and processable carbohydrate pulps. Energy Environ. Sci. *8,* 1748-1763.
22. Van den Bosch, S., Renders, T., Kennis, S., Koelewijn, S.-F., Van den Bossche, G., Vangeel, T., Deneyer, A., Depuydt, D., Courtin, C.M., Thevelein, J.M. et al. (2017). Integrating lignin valorization and bio-ethanol production: on the role of Ni-Al_2O_3 catalyst pellets during lignin-first fractionation. Green Chem. *19,* 3313-3326.
23. Shuai, L., Amiri, M.T., Questell-Santiago, Y.M., Heroguel, F., Li, Y., Kim, H., Meilan, R., Chapple, C., Ralph, J., and Luterbacher, J.S. (2016). Formaldehyde stabilization facilitates lignin monocyclic production during biomass depolymerisation. Science *354,* 329-333.
24. Lan, W., Amiri, M.T., Hunston, C.M., and Luterbacher, J.S. (2018). Protection group effects during α,β-diol lignin stabilization promote high-selectivity monocyclic production. Angew. Chem. Int. Ed. *57,* 1-6.
25. Shuai, L., Sitison, J., Sadula, S., Ding, J., Thies, M.C., and Saha, B. (2018). Selective C-C bond cleavage of methylene-linked lignin models and kraft lignin. ACS Catal. *8,* 6507-6512.
26. Ma, Z., Troussard, E., and Bokhoven, J. A. (2012). Controlling the selectivity to chemicals from lignin via catalytic fast pyrolysis. Appl. Catal. A: Gen. *423,* 130-136.
27. Jan, O., Marchand, R., Anjos, L.C.A., Seufitelli, G.V.S., Nikolla, E., and Resende, F.L.P. (2015). Hydropyrolysis of lignin using Pd/HZSM-5. Energy Fuels *29,* 1793-1800.
28. Mu, W., Ben, H., Ragauskas, A., and Deng, Y. (2013). Lignin pyrolysis components and upgrading-technology review. BioEnergy Res. *6,* 1183-1204.
29. Li, X., Su, L., Wang, Y., Yu, Y., Wang, C., Li, X., and Wang, Z. (2012). Catalytic fast pyrolysis of kraft lignin with HZSM-5 zeolite for producing aromatic hydrocarbons. Front. Env. Sci. Eng. *6,* 295-303.
30. Zhao, Y., Deng, L., Liao, B., Fu, Y., and Guo, Q-X. (2010). Aromatics production via catalytic pyrolysis of pyrolysis of pyrolytic lignins from bio-oil. Energy Fuels *24,* 5735-5740.
31. Vermeiren, W., and Gilson, J.P. (2009). Impact of zeolites on the petroleum and petrochemical industry. Top. Catal. *52,* 1131-1161.
32. Zhu, J., Meng, X., and Xiao, F.S. (2013). Mesoporous zeolites as efficient catalysts for oil refining and natural gas conversion. Front. Chem. Sci. Eng. *7,* 233-248.
33. Michaud, P., Lemberton, J.L., and PeÂrot, G. (1998). Hydrodesulfurization of dibenzothiophene and 4,6-dimethyldibenzothiophene: effect of an acid component on the activity of a sulfided NiMo on alumina catalyst. Appl Catal A: Gen *169*, 343-353.
34. Zhang, D., Duan, A., Zhao, Z., and Xu, C. (2010). Synthesis, characterization, and catalytic performance of NiMo catalysts supported on hierarchically porous Beta-KIT-6 material in the hydrodesulfurization of dibenzothiophene. J. Catal. *274,* 273-286.
35. Shao, Y., Xia, Q., Dong, L., Liu, X., Han, X., Parker, S.F., Cheng, Y., Daemen., L., Ramirez-Cuesta, A.J., Yang, S. and Wang, Y. (2017). Selective production of arenes via direct lignin upgrading over a niobium-based catalyst. Nat. Commun. *8,* 16104.
36. Xia, Q., Chen, Z., Shao, Y., Gong, X., Wang, H., Liu, X., Parker, S.F., Han, X., Yang, S., and Wang, Y. (2016). Direct hydrodeoxygenation of raw woody biomass into liquid alkanes. Nat. Commun. *7,* 11162.
37. Li, Y., Akiyama, T., Yokoyama, T., and Matsumoto, Y. (2016). NMR assignment for diaryl ether structures (4-O-5 structures) in pine wood lignin. Biomacromolecules *17,* 1921-1929.
38. Ma, R., Zhang, X., Wang, Y., and Zhang, X. (2018). New Insights Toward Quantitative Relationships between Lignin Reactivity to Monomers and Their Structural Characteristics. ChemSusChem *11*, 2146-2155.
39. Yamamura, M., Hattori, T., Suzuki, S., Shibata, D., and Umezawa, T. (2010). Microscale alkaline nitrobenzene oxidation method for high-throughput determination of lignin aromatic components. Plant Biotechnol J. *27*, 305-310.
40. Chui, M., Metzker, G., Bernt, C.M., Tran, A.T., Burtoloso, A.C.B., and Ford, P.C. (2017). Probing the lignin disassembly pathways with modified catalysts based on Cu-doped porous metal oxides. ACS Sustainable Chem. Eng. *5*, 3158-3169.
41. Miyazawa, T., Kusunoki, Y., Kunimori, K., and Tomishige, K. (2006). Glycerol conversion in the aqueous solution under hydrogen over Ru/C + an ion-exchange resin and its reaction mechanism. J. Catal. *240*, 213-221.
42. Fihri, A., Bouhrara, M., Patil, U., Cha, D., Saih, Y., and Polshettiwar, V. (2012). Fibrous nano-silica supported ruthenium (KCC-1/Ru): a sustainable catalyst for the hydrogenolysis of alkanes with good catalytic activity and lifetime. ACS Catal. *2*, 1425-1431.
43. Palkovits, R., Tajvidi, K., Procelewska, J., Rinaldi, R., and Ruppert, A. (2010). Hydrogenolysis of cellulose combining mineral acids and hydrogenation catalysts. Green Chem *12*, 972-978.
44. Rahimi, N., and Karimzadeh, R. (2011). Catalytic cracking of hydrocarbons over modified ZSM-5 zeolites to produce light olefins: a review. Appl Catal A: Gen *398*, 1-17.
45. Solca, N. and Dopfer, O. (2002). Protonated benzene: IR spectrum and structure of $C_6H_7^+$. Angew. Chem. Int. Ed. *41,* 3628-3631.
46. Parker, S.F., Fernandez-Alonso, F., Ramirez-Cuesta, A., Tomkinson, J., Rudic, S., Pinna, R., Gorini, G., and

Castanon, J. (2014). Recent and future developments on TOSCA at ISIS. J. Phys. Conf. Ser. *554*, 012003.

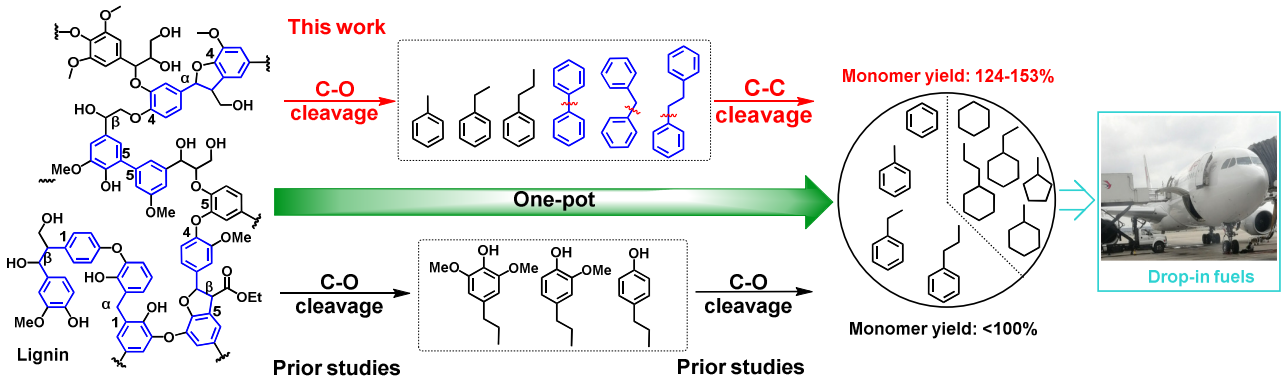

Figure 1. View of a representative structure of a lignin fragment, showing various intramolecular linkages and schematic representation of the one-pot depolymerisation and hydrodeoxygenation of lignin into monocyclic aromatic hydrocarbons.
The route above the green arrow shows the formation of monocyclic arenes via cleavage of both C-O and C-C linkages.

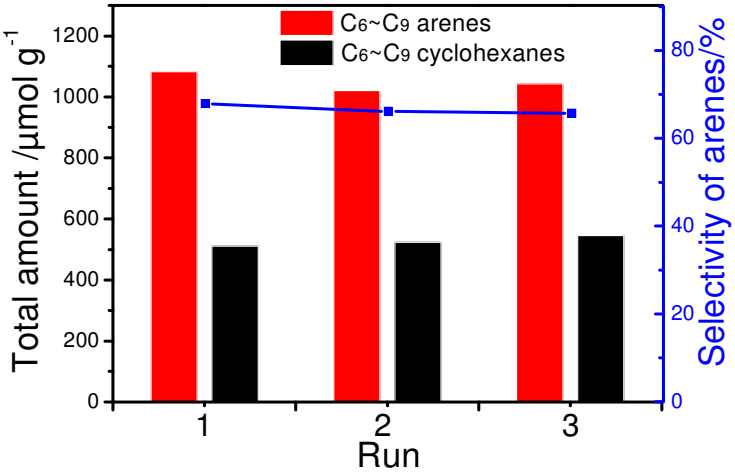

Figure 2. Comparison of C_6-C_9 reaction products and arene selectivity in three consecutive recycling runs of one-pot conversion of Kraft lignin over the Ru/$NbOPO_4$ catalyst.
Reaction conditions: Kraft lignin 0.1 g, Ru/$NbOPO_4$ 0.2 g, dodecane 5 mL, H_2 0.5 MPa, 310 °C for 40 h.

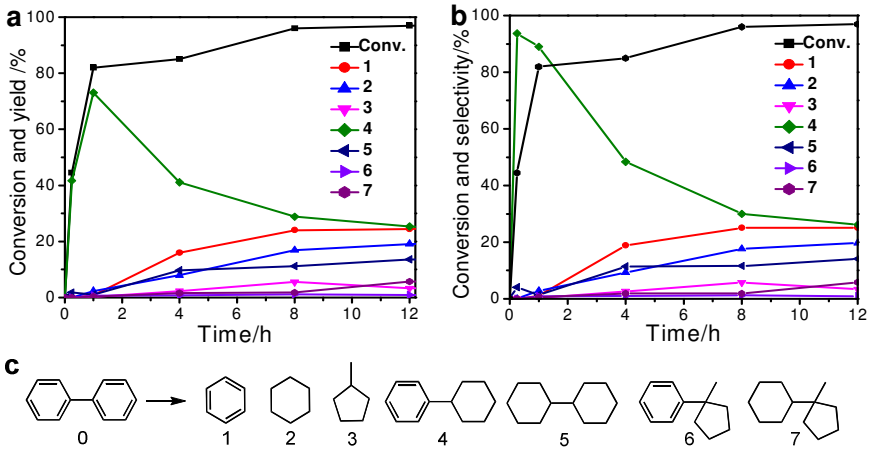

Figure 3. Product distributions versus reaction time for the conversion of biphenyl over the Ru/NbOPO$_4$ catalyst.
Views of variation of the yield (a) and selectivity (b) for all possible intermediates and products as shown in (c). Reaction conditions: biphenyl 0.2 g, 5% Ru/NbOPO$_4$ 0.1 g, dodecane 2 g, H_2 0.5 MPa, 280 ^oC.

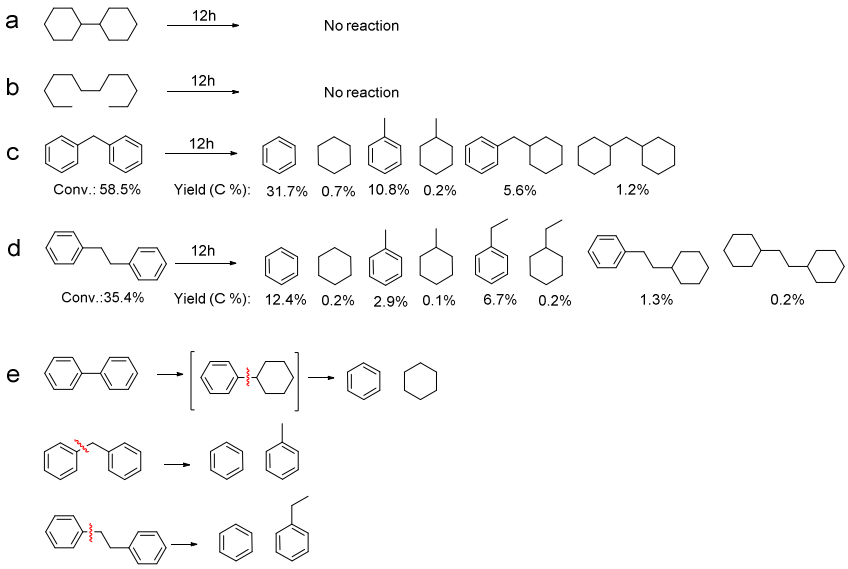

Figure 4. Product distributions for the conversion of bicyclohexyl (a), solvent dodecane (b), diphenylmethane (c), diphenylethane (d) and (e) schemes of selective hydrogenolysis of three lignin model compounds over the Ru/NbOPO$_4$ catalyst.
Reaction conditions: reactant 0.2g, 5% Ru/NbOPO$_4$ 0.1g, dodecane 2 g, H_2 0.5MPa, 280^{o}C, 12h. The yield of products was calculated using equations: Yield of the monocyclic compound = (molar amount of the monocyclic compound) / (molar amount of the substrate) / 2 × 100%; Yield of the bicyclic compound = (molar amount of the bicyclic compound) / (molar amount of the substrate) × 100%.

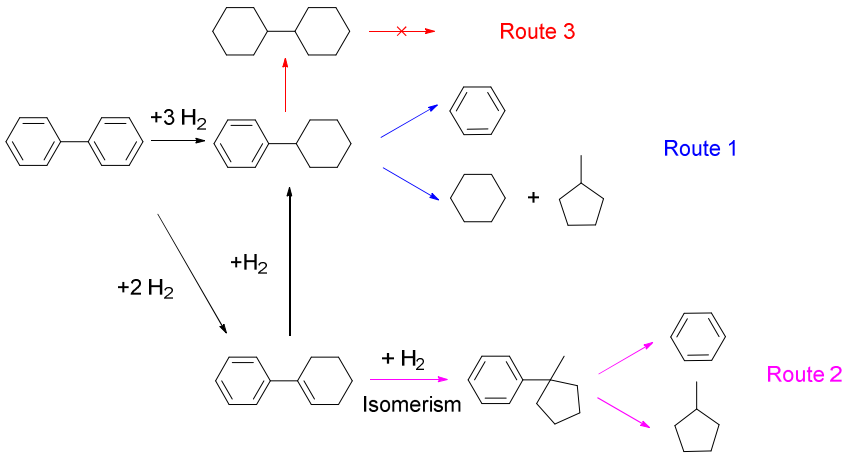

Figure 5. Proposed reaction network of the conversion of biphenyl over the Ru/NbOPO$_4$ catalyst.
The direct cracking of phenylcyclohexane in Route 1 is the dominant pathway.

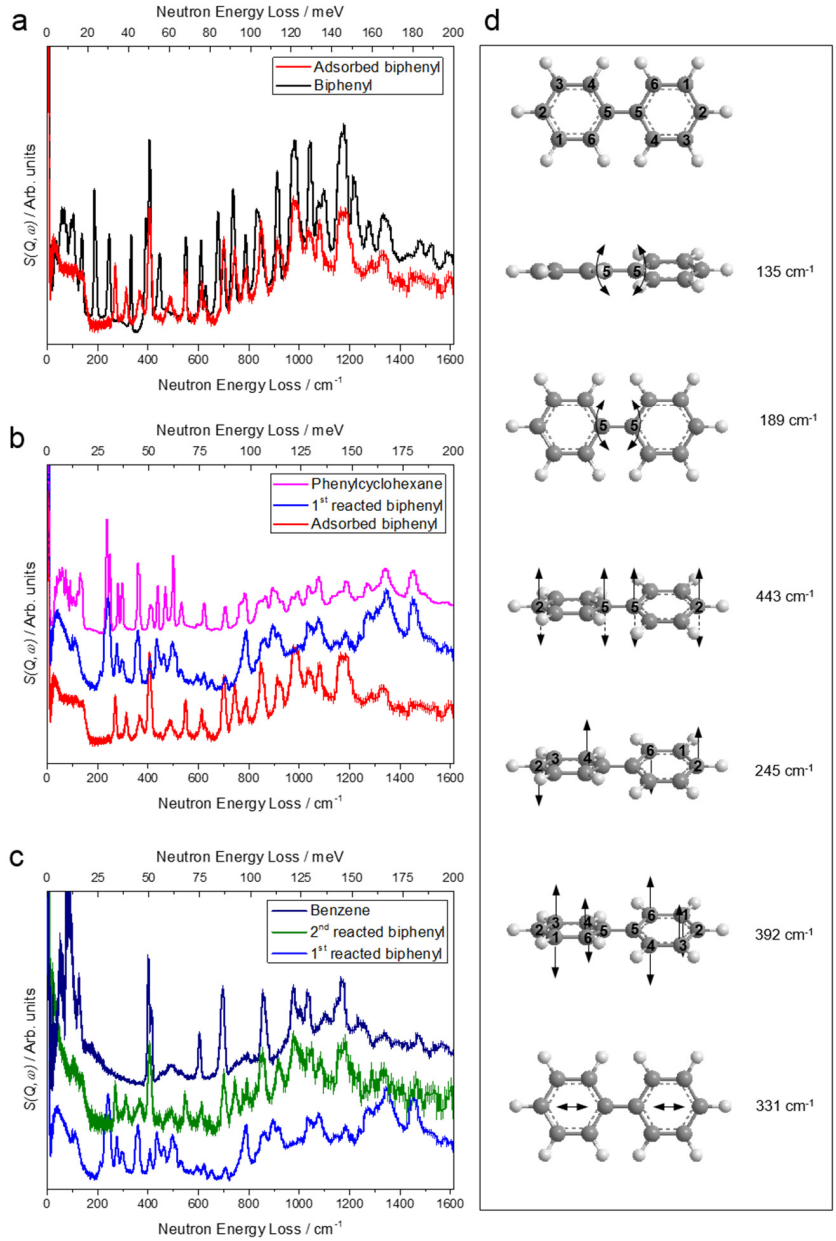

Figure 6. Inelastic neutron scattering (INS) spectra for Ru/NbOPO$_4$ on the adsorption and catalytic conversion of biphenyl.
All spectra shown here are difference spectra; raw data are shown in Figures S9 and S10. INS spectra of the reduced catalysts were used throughout for calculations of the corresponding difference spectra. No abscissa scale factor was used throughout this report for INS calculations. INS spectra for condensed biphenyl, phenylcyclohexane, and benzene in solid state at 10 K were included accordingly for a direct comparison of the vibrational modes between the adsorbed/bound molecules and the free, intact molecules. Two hydrogenation reactions of adsorbed biphenyl were conducted pure and diluted (5%) H_2 steam. Where no error bars are visible these are smaller than the symbols used to represent the data points. (a) Comparison of INS spectra for solid and adsorbed biphenyl on Ru/NbOPO$_4$. INS spectra for Ru/NbOPO$_4$ during the first (b) and second (c) catalytic conversion of biphenyl. (d) Views of selected C-C vibration models of biphenyl.

Table 1. Summary of the products distribution from the one-pot conversion of lignin over the Ru/NbOPO$_4$ catalyst[a]

Entry	Lignin	Products distribution (μmol·g^{-1})		Total amount (μmol g^{-1}/ wt %)	Selec. to arenes (%)[c]	RMY (%)[d]
		C6-C9 arenes	C6-C9 □y□loalkanes			

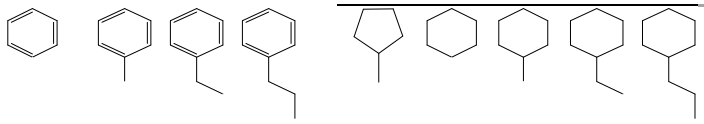

1	Kraft	524	389	103	67	209	42	167	67	26	1594/14.5	68	153
2[b]	Kraft	204	262	146	42	56	88	150	88	19	1055/10.1	62	101
3	Enzymic	651	323	387	77	69	98	203	266	61	2135/20.3	67	147
4	Pine	1179	640	177	138	285	211	448	111	65	3254/29.3	66	151
5	Birch	796	877	251	191	254	191	487	189	158	3394/31.9	62	124

[a]Reaction conditions: lignin (0.1 g), 5%Ru/$NbOPO_4$ (0.2 g), dodecane (5 mL), H_2 0.5 MPa, 310ºC, 40h.
[b]Reaction conditions: lignin (0.1 g), 5%Ru/$NbOPO_4$ (0.2 g), dodecane (5 mL), H_2 0.5 MPa, 250ºC, 20h.
[c]Selectivity to arenes = (total amount of arenes) / (total amount of hydrocarbons) ×100%.
[d]Ratio of molar yields (RMY) = (molar yield of monocyclic compounds over Ru/$NbOPO_4$) / (molar yield of monocyclic compounds from NBO) × 100% = (total amount of monocyclic hydrocarbons over Ru/$NbOPO_4$) / (theoretical amount of monocyclic hydrocarbons from NBO) ×100%. Theoretical hydrocarbons amount of Kraft lignin, enzymic lignin, pine lignin and birch lignin is 1040, 1448, 2162 and 2741 μmol g^{-1}, respectively. Theoretical hydrocarbons amount is calculated using the NBO method as described in Table S2 and Note S1.

Table 2. Summary of the products yields from the conversion of biphenyl over different catalysts[a]

Entry	Catalyst	Yield (C %)[d]							Conv. (C %)
		Monocyclic			Dicyclic				
		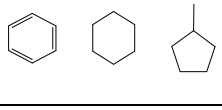			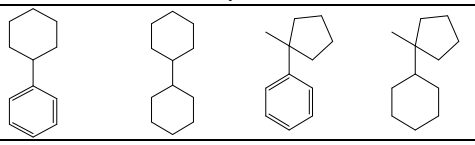				
1	5%Ru/$NbOPO_4$	24.4	19.1	3.3	25.4	13.6	0.9	5.7	97.0
2	5%Ru/Nb_2O_5	1.1	2.3	0.1	55.8	24.2	0.5	4.9	97.8
3[b]	5%Ru/Nb_2O_5 TfOH	20.1	5.0	12.9	29.8	15.7	0.2	2.0	98.2
4	$NbOPO_4$	0	0	0	0	0	0	0	0
5	5%Pd/$NbOPO_4$	16.3	12.3	3.6	5.5	42.1	3.1	6.6	>99.9
6	5%Pt/$NbOPO_4$	1.3	18.5	1.4	2.1	54.2	1.7	5.6	>99.9
7	5%Rh/$NbOPO_4$	3.5	33.6	2.3	21.7	15.8	2.7	7.5	98.8
8[c]	5%Ru/HZSM-5	4.9	3.1	0.8	57.3	4.7	1.4	0.3	95.3

[a]Reaction conditions: biphenyl (0.2 g), catalyst (0.1 g), dodecane (2 g), H_2 0.5 MPa, 280ºC, 12h.
[b]Reaction conditions: biphenyl (0.2 g), catalyst (0.1 g), trifluoromethanesulfonic acid (0.05g) dodecane (2 g), H_2 0.5 MPa, 280ºC, 12h.
[c]C_1-C_4 alkanes were detected in the gas phases.
[d]The yield of products was calculated using equations: Yield of the monocyclic compound = (molar amount of the monocyclic compound) / (molar amount of the substrate) / 2 × 100%; Yield of the bicyclic compound = (molar amount of the bicyclic compound) / (molar amount of the substrate) × 100%.